Science and Technology Indonesia
e-ISSN:2580-4391 *p*-ISSN:2580-4405
Vol. 7, No. 4, October 2022

Research Paper

Prediction of Ground Surface Deformation Induced by Earthquake on Urban Area Using Machine Learning

Fathoni Usman[1]*, Nanda[2], Josaphat Tetuko Sri Sumantyo[3]

[1]*Institute of Energy Infrastructure, Universiti Tenaga Nasional, Selangor, 43000, Malaysia*
[2]*Department of Civil Engineering, Faculty of Engineering, Universitas Putra Indonesia, Padang, 25145, Indonesia*
[3]*Centre for Environmental Remote Sensing, Chiba University, Chiba, 2638522, Japan*
***Corresponding author**: fathoni@uniten.edu.my

Abstract
Earthquakes can inflict significant damage to structures and infrastructures. This paper presents a machine learning model to predict ground surface deformation (GDS) induced by earthquake events. The data on historical GSD is extracted from radar product of Synthetic Aperture Radar (SAR) data of one-year over five magnitude earthquakes that occurred within 200 kilometers of the Kota Padang Regency, West Sumatra. Building topology data of its footprint area, distance from shoreline, elevation, and coordinate were incorporated as the main features in the dataset. The earthquake parameters were taken from the USGS earthquake data catalog. Four machine learning algorithms of Neural Network (NN), Random Forest (RF), k-Nearest Neighbors (kNN), and Gradient Boosting (GB) are applied. The GSD from the trained models is predicted and compared with the measured GSD from the SAR's product. The performances of proposed algorithms are evaluated in terms of the statistical index. A new dataset from the earthquake event in March 2022 is used to predict the GSD and further test the performance of the trained models. Overall, the four machine learning algorithms have outstanding performance, with a coefficient determinant of more than 0.9. The kNN algorithm outperforms compared to others in delineating the GSD. The trained models gave deficient prediction performance on the new dataset with a correlation coefficient of 0.228 predicted by the RF algorithm. Additional earthquake datasets and more unique features will improve the performance of the machine learning algorithms.

Keywords
Machine Learning, Ground Surface Deformation, Vulnerability, Earthquake

Received: 13 April 2022, Accepted: 27 August 2022
https://doi.org/10.26554/sti.2022.7.4.435-442

1. INTRODUCTION

Sumatra is on the Sunda Plate, which runs parallel to the Indo-Australian plate. The Australian plate regulates the region's seismicity beneath the Eurasian plate with a 14 mm/year subduction velocity. Sumatra Island also endures a 50 to 60 mm/year oblique convergence velocity from the plate and a 23 mm/year geodetic slip across the Great Sumatra Fault (GSF) (Triyoso et al., 2020). Furthermore, the Mentawai Fault Zone's forearc runs parallel to the GSF as a separate microplate or sliver plate across Sumatra Island. The distances between Sumatra Fault Zone (SFZ) and Mentawai Fault Zone (MFZ) are approximately 80 km and 120 km, respectively, to Padang City's urban area. Padang City is in an area prone to major earthquakes and their associated secondary consequences, such as tsunamis. More than 200 earthquakes over 5.0 magnitude from 2000 to 2022 were recorded in the USGS earthquake data catalog (USGS, 2022).

The most critical effort in developing a response plan to natural disasters related to an earthquake is to characterize the spatial sources of earthquakes and the seismic hazard due to seismic amplification and understand the threat from the earthquakes to people, buildings, and infrastructure. The ground surface deformation (GSD) naturally happens due to an isostatic load of Holocene deposits from sediments and natural compactions or as a consequence of tectonic and volcanic activities (Hamim et al., 2019). A study on determining the GSD based on radar data of Sentinel 1 in the Padang City area has been conducted (Usman et al., 2022). The vulnerability of buildings based on GSD has been determined by using the unsupervised K-Mean cluster analysis to classify the GSD in the Kota Padang Regency (Usman, 2021). Both studies have good agreement on mapping the most responsive area to the ground deformation related to the liquefaction during the earthquake of September 2009 (Adji et al., 2021). Liquefaction has occurred in some areas of the Kota Padang Regency, which relates

to the high sand content and high-water table present along the low coastal strip plain of the region.

The traditional methods of post-earthquake building assessment, which include an extensive in-situ building-by-building study by structural engineers, are becoming less capable of dealing with larger built-up areas (Mangalathu et al., 2020). In recent years, remote sensing has extracted significant aspects for large areas' pre-event vulnerability analyses of built-up structures. Its great potential has been demonstrated (Geiß et al., 2015; Usman, 2021). The Sentinel-1A satellite technology was utilized to acquire high-resolution co-seismic surface displacement data and compared with the linear and nonlinear inversion techniques of an elastic half-space dislocation model. The results indicated that the model could describe the surface deformation well (Qiu and Qiao, 2017). The Mogi model assumes the Earth's crust is a partly infinite elastic substance, displacing its surface by changing pressure or volume. The Yang model builds on Mogi's symmetrical, spherical point source. The two models were compared with inversion techniques of an elastic half-space dislocation model and long-term data from a global positioning system (GPS) on surface deformation data (Mattioli et al., 2010). The Mogi and Yang models were used to match actual displacements recorded after a seismic earthquake using satellite radar data based on fundamental indicators of subsidence, slope, curvature, horizontal displacements, and horizontal deformations (Milczarek et al., 2021; Meng et al., 2022).

The recent techniques of processing and analyzing the earthquake data, its impact on the structural and non-structural assets, and the hazard level have been studied using machine learning (Xiong et al., 2021). Machine Learning (ML) is a branch of Artificial Intelligence (AI). It deals with a computational process that can learn from data, find patterns, and decide independently. The ML has made significant advancements in its capability to tackle complex problems in data science in a range of diverse fields of knowledge, including material science, air pollution studies, and environmental engineering (Xie et al., 2020). The application of AI and ML was utilized to predict the service life of building components in different environmental loads (Tapir et al., 2005) and classify the earthquake hazard on RC buildings (Harirchian et al., 2021). Earthquake engineering studies the hazard in determining how the earthquake damages the site and structures to mitigate and prevent their effects. Typically the study is underpinned by four objectives: activity to reduce long-term disaster, disaster preparedness, adaptation and response plan, and post-disaster recovery plan (Jiao and Alavi, 2020; Harirchian et al., 2021). Machine learning in earthquake engineering is utilized mainly in hazard analysis, damage detection, and seismic vulnerability evaluation to determine how resilient the system is and damage prevention of a structural system. Thirty years of data on the earthquakes' location, depth, and magnitude were used to predict earthquake events in Indonesia and compare three different machine learning algorithms (Murwantara et al., 2020). Utilizing 123 datasets with eight variables, Artificial Neural Network (ANN) was used to predict the number of damaged buildings and casualties due to earthquakes in Indonesia (Oktarina et al., 2020).

This paper presents an effort to predict the ground surface deformation induced by over 5.0 magnitude earthquakes in combination with the InSAR product of vertical displacement of the ground using several ML methods. The effort to determine the vulnerability of buildings based on the material and structural type and determine the building damage level by operating machine learning method for the West Sumatra region and Padang City has been conducted (Geiß et al., 2015; Sari et al., 2019; Sari et al., 2021). Data mainly were taken based on the 30^{th} September 2009 major earthquake. Machine learning was used to assess seismic building structural types (SBSTs) and map the earthquake-prone area using data from multispectral IKONOS, multitemporal LANDSAT, and Sentinel-1 radar data. (Geiß et al., 2015; Usman, 2021). It gave a better understanding of the possible impact of the earthquake on the buildings.

2. EXPERIMENTAL SECTION

2.1 Study Area

Figure 1 shows the earthquake events that mostly happened in the forearc basin of the MFZ. Figure 2 shows the fault zones and the subduction trench on the bathymetry of the seafloor between Sumatra Island and Mentawai Island. On 30^{th} September 2009, three earthquakes with moment magnitudes of Mw 7.6 (at 5:16:10 PM local time), Mb 5.8 (at 5:19:33 PM), and Mb 5.4 (at 5:38:52 PM) struck off the west coast of Sumatra near Kota Padang Regency and Pariaman Regency, killing 1,195 people and destroying over 180,000 structures, including schools and 272 health facilities. Three hundred eighty-three people died, and 431 were critically injured in Kota Padang Regency, mainly because of collapsed structures.

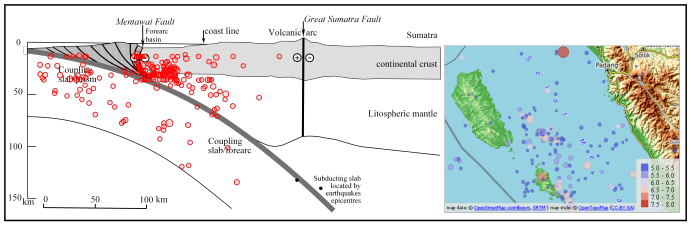

Figure 1. Over 5.0 MW Magnitudes of Earthquakes from January 2000 to February 2022 Overlaid on the Mentawai Fault Zone.

In earthquake-prone areas, increasing the spatial concentration of exposed factors such as people, buildings, infrastructure, or economic values increases the seismic risk to unprecedented levels. In September 2009's earthquakes, soil settlement, and liquefaction occurred. In many cases, building foundations were distorted due to lateral movements and differential settlements, so the buildings will need to be rebuilt (Bothara et al., 2010; Rahardjo et al., 2014; Chian et al., 2019). Kota Padang

Table 1. Over 5.0 Magnitude Earthquake from August 2020 to the End of February 2022

Earthquake	Latitude	Longitude	Depth (km)	Magnitude (MW)	Bperp (m)	Btemp (days)
24/02/2022	0.2331	100.1058	12.34	6.2	15	24
12/09/2021	-0.5281	99.7137	35	5.4	4	24
05/05/2021	-1.9554	99.7862	30	5.7	15	24
02/05/2021	-2.3244	99.79	21	5.5		
05/03/2021	-1.7567	99.2329	25	5.6	25	12
18/11/2020	-1.8125	100.4271	15.62	5.2	5	12
04/08/2020	-1.7797	100.1815	48.42	5.1	23	24

Regency had a 6.55% organized housing area in 2021. Between 2020 and 2021, there is an increase of 8.2%, or more than 500 hectares of new open land for residential housing, replacing the irrigated farming land. Informal, disorganized, and highly susceptible settlements arose due to the city's rapid growth (BPS-Statistics of Padang Municipality, 2022).

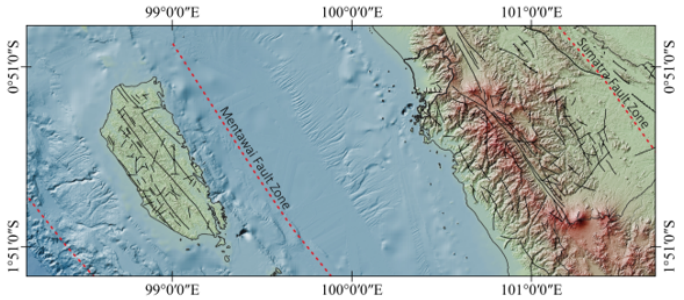

Figure 2. The Fault Lines, the Sumatra Fault Zone (SFZ) and the Mentawai Fault Zone (MFZ), with the Seafloor Bathymetry of the Strait Between the Islands (Badan Informasi Geospasial, 2018)

The interior of the Kota Padang Regency is made up of tertiary sedimentary rocks, whereas the surface is made up of metamorphic rocks. The alluvial plain is about 10 km broad east-west and 20 km wide north-south, and it wraps around the foot of the mountains. Figure 3 shows the geological formation of the Kota Padang Regency with several fault lines delineated mainly on the hilly terrain area. The soil is composed of sediments and loose soil eroded and carried downstream by a flood or a river. The geology of the coastal area is characterized by loose sand deposits, gravel with discontinuous silt and clay layers, and certain water-saturated areas (Muin and Nawir, 2011). The deposit source zone dominates the coastal embankment span on the northwest side. During the 2009 earthquake, liquefaction occurred in some portions of the Kota Padang Regency, which was caused by the high sand content and high-water table widespread along the region's low coastal strip plain (Hakam et al., 2020).

2.2 Datasets

The footprint area of the building is extracted from open street map (OSM) building data accessed from overpass-turbo.eu.

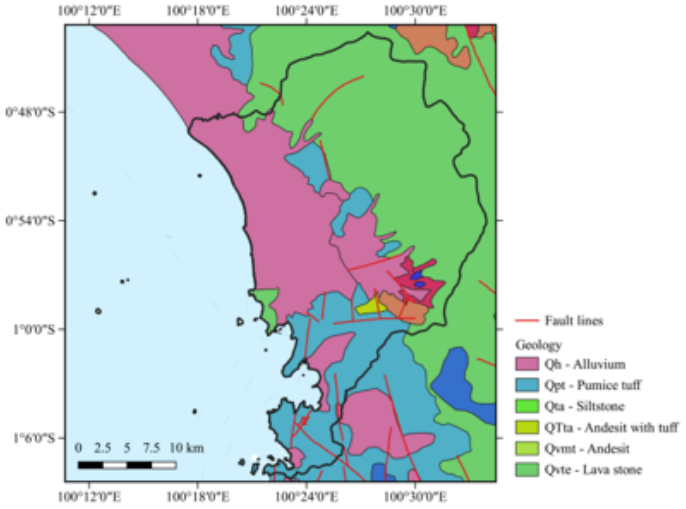

Figure 3. The Geological Formation of Kota Padang Regency

There are about 145,000 building footprints within the study area. The digital elevation model of DEMNAS is used to determine the elevation. We extracted the elevation data using the centroid of the building footprint. The SAR radar data of Sentinel-1 satellite from pre- and post-earthquake events over 5.0 magnitude are used to get the surface deformation data. The selection of the magnitude of the earthquake less than 5.0 magnitude were not included based on the peak ground acceleration (PGA) that traveled on to the study area is very low (< 0.05%), and the intensity scale is I (i.e., the shaking was not felt). The GSD is part of the InSAR product package processed by Alaska Satellite Facilities (ASF) using GAMMA software (ESA, 2022). The pairs of radar imageries are selected using SBAS (Small Baseline Subset) in the ASF Vertex online data search (search.asf.alaska.edu). Figure 4 shows the InSAR product from pairs of SAR data for the vertical displacement and wrap interferometry of the earthquake on 24th February 2022 at Pasaman Barat, West Sumatra. Manual processes of InSAR have been used and explained in other articles (Hamim et al., 2019; Usman, 2021). Table 1 lists the earthquake events and the baseline information of pairs of radar imageries: the perpendicular baseline (B_{perp}) and temporal baseline (B_{temp}).

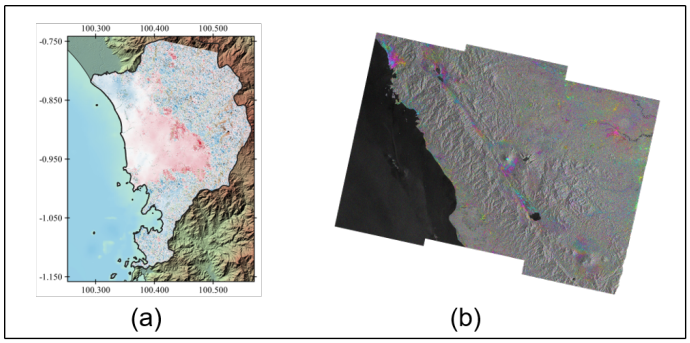

Figure 4. (a) The InSAR Product of Vertical Displacement, (b) The Wrapped Interferogram Phase from Pairs of Radar Data on Earthquake Events on 24th February 2022 (ESA, 2022)

2.3 Methods

The parameters related to the building topology are the nearest distance of the building from the shoreline (X_{Dslm}), building footprint's area (X_{Am2}), presuming they are single-story buildings, elevation of the building (X_{Elm}), and the building location (X_{Lat}, X_{Long}). Factors that are connected to the ground surface deformation induced by the earthquakes are the ground surface deformation ($G_{SDispmm}$), the earthquake magnitude (X_{MagMw}), the depth ($X_{Depthkm}$), the distance of the building from the hypocentre (X_{HypDkm}), and the bearing of the earthquake to the building's location ($X_{Bearing}$). The earthquake data was taken from the USGS earthquake catalog. The conceptual machine learning framework is presented in Figure 4. Figure 5 shows the location of over 5.0 magnitude earthquakes and their direction toward the Kota Padang Regency.

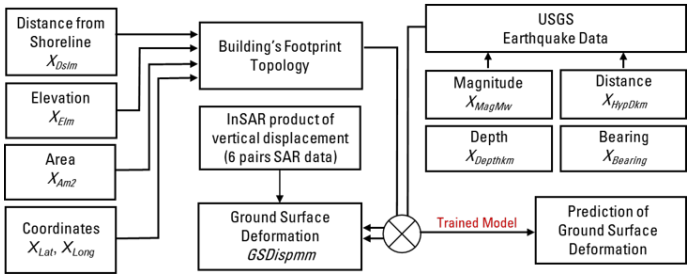

Figure 5. The Conceptual Machine Learning Framework of the GSD

Four machine learning algorithms are used as the regressor in this study, namely k-Nearest Neighbors (kNN), Random Forest (RF), Gradient Booster (GB), and Neural Network (NN). Random Forest is a regression approach that uses ensemble learning. It is an approach that requires combining numerous trees with similarly distributed and equally weighted individual trees. The final model is based on a majority vote among the forest's individually produced trees. The Gradient Boosting is an algorithm that involves gradually boosting the prediction function F_b by adding the estimator S. The learning process

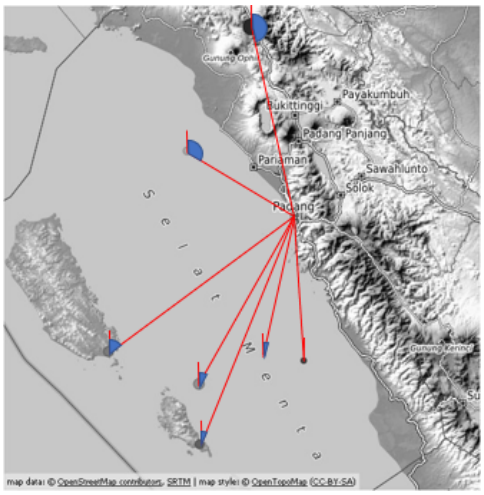

Figure 6. The Bearing of Each Earthquake to the Building's Location at Kota Padang Regency That Used in Machine Learning ($X_{Bearing}$).

begins when the S is fitted to the (y–F_b) residual. The F_{b+1} is modified to minimize error values at each step as in (1) (Hanoon et al., 2021).

$$F_{b+1}(x) = F_b(x) + S = y - F_b(x) \quad (1)$$

The kNN algorithm relies on distance for classification. The neighbor parameter for the kNN algorithm in this study is 20, with Euclidean and Distance selected for the metric and the weight, respectively. The NN algorithm uses a multi-layer perceptron (MLP) algorithm with backpropagation. We use the Rectified Linear Unit (ReLU) with Adam as the activation function and solver algorithm for the NN with two layers of 50 and 100 nodes. The implementation of the machine learning algorithms is processed in the Orange Data Mining software version 3.32.0 (Demšar et al., 2013). The hardware used in this study is a mobile workstation with Intel Xeon E-2176M CPU at 2.71 GHz in a 64-bit operating system x64-based processor and 64 GB RAM.

2.4 Statistical Evaluation

The developed prediction model's performance should be evaluated and compared to other models (Azarakhsh et al., 2022; Naghibi et al., 2022; Guo et al., 2020). We use statistical indices to determine which model outperformed the others. It should be highlighted that each statistical index only looks at the model's outputs concerning the target values. The prediction result is evaluated based on four criteria: mean absolute error (MAE), mean square error (MSE), root mean square error (RMSE), and coefficient of determination (R^2). One dataset of earthquake events from the trained dataset was fed into the training and testing process to evaluate the prediction results over the GSD data of the trained model. The statistical indices are calculated as below:

Table 2. Comparison of Performance of the Machine Learning Algorithms

Model	Train Time (s)	Test Time (s)	MSE	RMSE	MAE	R^2
Gradient Boosting	440.081	0.292	4.54E-06	0.002	0.001	0.988
kNN	81.976	27.293	3.51E-05	0.006	0.004	0.904
Random Forest	2246.779	3.839	1.06E-05	0.003	0.002	0.971
Neural Network	1344.613	5.704	2.92E-06	0.002	0.001	0.992

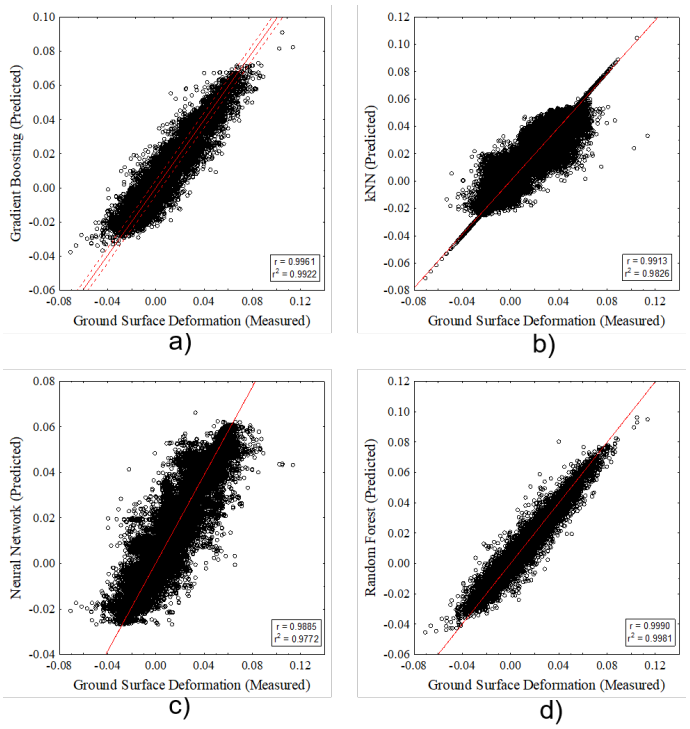

Figure 7. The Measured and Predicted GSD for (a) GB, (b) kNN, (c) NN, and (d) RF

$$RMSE = \sqrt{\frac{1}{n}\sum_{i=1}^{n}(M_i - P_i)} \quad (2)$$

$$MAE = \frac{1}{n}\sum_{i=1}^{n}|Mi - Pi| \quad (3)$$

$$MAE = \frac{1}{n}\sum_{i=1}^{n}(Mi - Pi)^2 \quad (4)$$

$$R^2 = 1 - \frac{SS_{res}}{SS^{tot}}; SS^{res} = \sum_{1}(Mi - Pi)^2; SS^{tot} = \sum_{1}(Mi - \bar{M})^2 \quad (5)$$

where P_i is the predicted value for the i^{th} case; M_i is the measured value of GSD from the InSAR product for the i^{th} ; $\bar{M}$ is the average of the measured values; i is the index of measured values ranging from 1 to n; SS_{tot} is the total sum of squares, and SS_{res} is the residual sum of squares.

Further performance evaluation of the trained model is conducted by providing a new dataset to the trained model from the earthquake on 13^{th} March 2022, which is located at latitude -0.63 and longitude 98.6294 at 28 km depth, 190 km to the epicenter. Plotting the measured and predicted GSD values allows for qualitative analysis of the machine learning trained model's prediction results (Zhou et al., 2021).

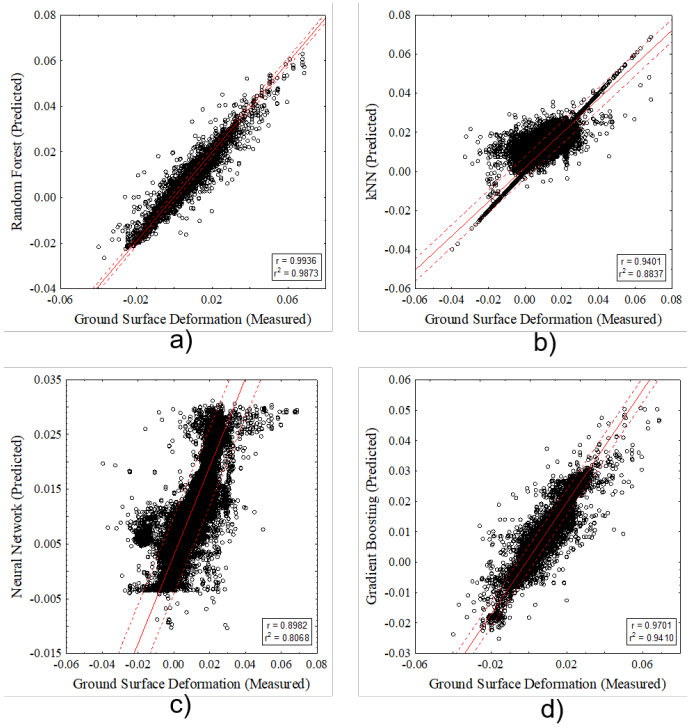

Figure 8. The Measured and Predicted GSD for (a) RF, (b) kNN, (c) NN, and (d) GB of the May 2021 Dataset

3. RESULT AND DISCUSSION

This paper is aimed to predict the ground surface deformation induced by over 5.0 magnitude earthquakes using machine learning. The dataset consists of building topology and earth-

quake information. One dataset consists of about 145,000 numerical types of data with nine input variables and one single output variable to predict. It gave a total instance of more than 868,000 to process. The data with no defined value, which occurred due to clipping the raster data of the InSAR product with a resolution of 80 m, were cleaned before the default preprocess data. The preprocess was applied using standardize to μ=0 and σ^2=1. The dataset was divided into 80% for training and 20% for testing the model. The training process of RF and NN algorithms took longer than the GB. The kNN algorithm took the fastest and is considered a lazy algorithm, and it took longer to test the trained model. Comparing the performance of four machine learning algorithms statistically shows that all the algorithms come out with the value of the coefficient of determinant over 0.9 considered very high performance. The GB and NN algorithms outperform compared to other algorithms. Table 2 list the statistical indexes to compare the performance of each machine learning algorithm.

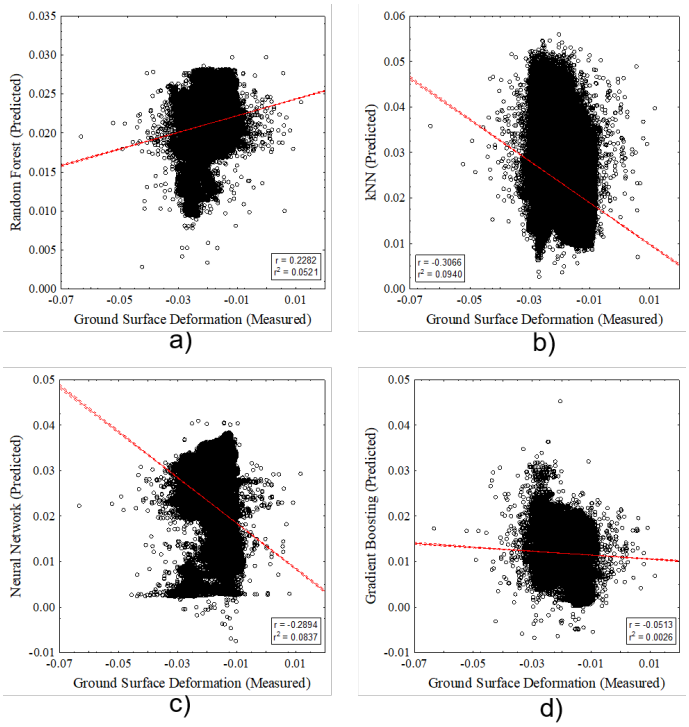

Figure 9. The Measured and Predicted GSD for (a) RF, (b) kNN, (c) NN, and (d) GB of the New Dataset for March 2022

To evaluate the trained machine learning algorithm's performance, we retrieved a dataset of an earthquake occurrence in May 2021 from the trained model's dataset. The dataset is fed to be processed using the trained model. It is observed that even though the algorithm was excellent, the results of the GSD prediction were not consistent. A scatter plot between measured and predicted values is plotted in Figure 7 to observe relationships between the values. It is observed that the kNN algorithm gave an excellent delineation qualitatively of predicted GSD when it plotted to the map of Kota Padang Regency as in Figure 8.

Table 3. Performance Comparison of the Trained Model to a New Dataset of an Earthquake on 13th March 2022

Model	MSE	RMSE	MAE	R^2
Gradient Boosting	0.001	0.033	0.032	0.0026
kNN	0.002	0.040	0.039	0.0940
Neural Network	0.002	0.043	0.041	0.0837
Random Forest	0.002	0.043	0.042	0.0521

A new dataset of earthquake events on 13th March 2022 is fed into the trained model to predict the GSD. It is shown that a poor prediction has resulted. Table 3 and Figure 9 show the statistical evaluation result of the prediction compared to the measured GSD from the InSAR product. The qualitative analysis delineates the spatial distribution on the map, showing that the predicted GSD is scattered mainly on the positive value of the surface deformation. The Pearson distance is used in distance calculation to evaluate the distance between values of measured GSD and predicted GSD, as in Figure 11.

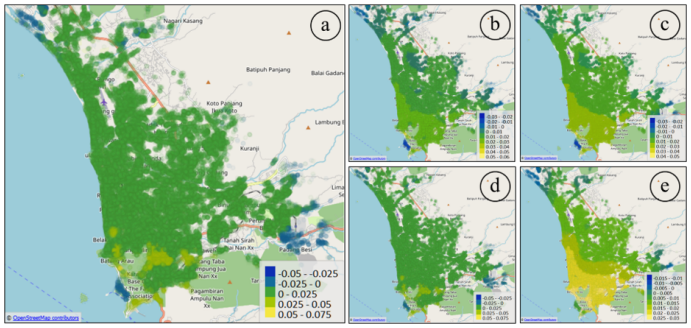

Figure 10. Qualitative Analysis of (a) the Measured GSD (the Unit is in Meters) from the InSAR Product of the May 2021 Earthquake Compared with Predicted GSD from the Trained Model of (b) GB, (c) RF, (d) kNN, and (e) NN

The Distance map using Pearson correlation describes the performance of the predicted GSD to the measured GSD. In Figure 11, it is shown that the closer the distance, the darker the grayscale color. The predicted GSD from the new dataset shows its broader range of distance among the machine learning algorithms. The poor performance of the trained machine learning model to predict the GSD on a new dataset derived from the less historical earthquake data induced the GSD. The additional variable tied explicitly to the study area needs to be added. Other researchers used data on peak ground acceleration (PGA), earthquake intensity, and peak spectral acceleration (PSA) for 0.3 seconds (Xie et al., 2020). The earthquake data in this paper relies on earthquake data from the USGS catalog. The detailed data on the ShakeMap is available when the earthquake's magnitude is over 5.5. The performance of ML prediction models for an earthquake study is based on the data.

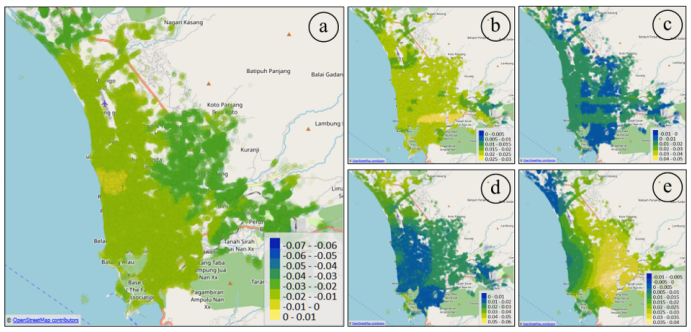

Figure 11. Qualitative Analysis of (a) the Measured GSD (the Unit is in Meters) from InSAR Product of 13th March 2022 Earthquake Compared with Predicted GSD from Trained Model (b) GB, (c) RF, (d) kNN, and (e) NN

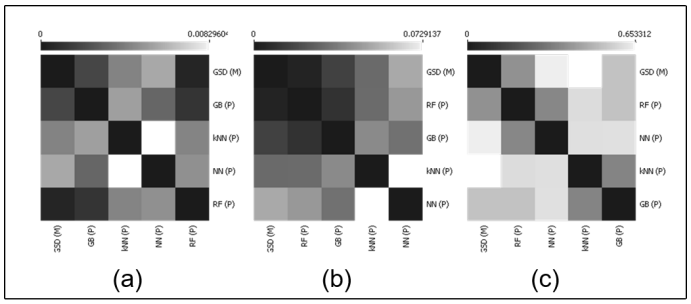

Figure 12. The Pearson's Distance Map Analysis Results on Three Different Datasets to Evaluate the Prediction Performance of the Trained ML's Model: (a) Distance Map of 6 Datasets, (b) Distance Map of the Dataset on the May 2021 Earthquake, and (c) Distance Map of the Dataset on March 2022 Earthquake

The location dictates the reliability and durability of earthquake monitoring systems and is essential to the prediction models (Jiao and Alavi, 2020).

4. CONCLUSION

This paper presents the use of Machine Learning (ML) in predicting GSD induced by over magnitude 5.0 Mw earthquake in Kota Padang Regency. Six GSD datasets were extracted from the InSAR product of vertical displacement from pairs of SAR data taken before and after the earthquake. Four ML algorithms were used to generate a trained model for the prediction. The performance of four ML algorithms is excellent, with its coefficient of determination above 0.9. When one dataset from the trained model was fed into the trained models, it was observed that the kNN algorithm gave a reasonable degree of accuracy for the ground surface distribution compared to other algorithms in terms of the spatial distribution of the predicted values of GSD. When a new dataset is fed into the trained model, it is observed that the prediction has deficient performance with a correlation value of 0.228 and a coefficient determination of 0.052. It indicates that unique variables that are currently used were not adequate. The variation direction ($X_{Bearing}$) of the earthquake in the study area is limited. More detailed earthquake data for the study area is of utmost importance to increase the ML models' performance. From this study, the ML has a promising potential to be used to predict the future GSD earlier without waiting for remote sensing data with a temporal resolution of 6 days to 12 days.

5. ACKNOWLEDGMENT

The authors would like to thank Universiti Tenaga Nasional for the Publication Grant of BOLD 2022, Universitas Putra Indonesia YPTK Padang for the PDP research grant 2021, and the Centre for Environmental Remote Sensing (CEReS), Chiba University, for the CEReS Overseas Joint Research Program 2021 (ID: CI21-111).

REFERENCES

Adji, B., B. Istijono, A. Hakam, S. Andriani, and M. Anshari (2021). Liquefaction Disaster Mitigation on Railway Corridors in Padang City, West Sumatra. *IOP Conference Series: Earth and Environmental Science*, **708**; 012025

Azarakhsh, Z., M. Azadbakht, and A. Matkan (2022). Estimation, Modeling, and Prediction of Land Subsidence Using Sentinel-1 Time Series in Tehran Shahriar Plain: A Machine Learning Based Investigation. *Remote Sensing Applications: Society and Environment*, **25**; 100691

Badan Informasi Geospasial (2018). DEMNAS Seamless Digital Elevation Model (DEM) dan Batimetri Nasional. Badan Informasi Geospasial

Bothara, J., D. Beetham, D. Brunsdon, M. Stannard, R. Brown, C. Hyland, W. Lewis, S. Miller, R. Sanders, and Y. Sulistio (2010). General Observations of Effects of the 30th September 2009 Padang earthquake, Indonesia. *Bulletin of the New Zealand Society for Earthquake Engineering*, **43**(3); 143

BPS-Statistics of Padang Municipality (2022). *Padang Municipality in Figures*. Padang, Indonesia: BPS-Statistics of Padang Municipality

Chian, S., S. Wilkinson, J. Whittle, R. Mulyani, J. Alarcon, A. Pomonis, K. Saito, S. Fraser, K. Goda, and J. Macabuag (2019). Lessons Learnt From the 2009 Padang Indonesia, 2011 Tōhoku Japan and 2016 Muisne Ecuador Earthquakes. *Frontiers in Built Environment*, **5**; 73

Demšar, J., T. Curk, A. Erjavec, Č. Gorup, T. Hočevar, M. Milutinovič, M. Možina, M. Polajnar, M. Toplak, A. Starič (2013). Orange: Data Mining Toolbox in Python. *The Journal of Machine Learning Research*, **14**(1); 2349–2353

ESA (2022). *Contains Modified Copernicus Sentinel Data [2020-2022]*. ESA

Geiß, C., P. A. Pelizari, M. Marconcini, W. Sengara, M. Edwards, T. Lakes, and H. Taubenböck (2015). Estimation of Seismic Building Structural Types Using Multisensor Remote Sensing and Machine Learning Techniques. *ISPRS Journal of Photogrammetry and Remote Sensing*, **104**; 175–188

Guo, Y., S. Hu, W. Wu, Y. Wang, and J. Senthilnath (2020).

Multitemporal Time Series Analysis Using Machine Learning Models for Ground Deformation in the Erhai Region, China. *Environmental Monitoring and Assessment*, **192**(7); 1–6

Hakam, A., D. Febriansyah, and B. M. Adji (2020). Liquefaction Mapping Procedure Development: Density and Mean Grain Size Formulations. *Geomate Journal*, **18**(70); 155–161

Hamim, S. A., F. Usman, et al. (2019). Determination of Land Subsidence Caused by Land Use Changing in Palembang City using Remote Sensing Data. *Third International Conference on Sustainable Innovation 2019 Technology and Engineering (IcoSITE 2019)*. Atlantis Press; 101–106

Hanoon, M. S., A. N. Ahmed, N. Zaini, A. Razzaq, P. Kumar, M. Sherif, A. Sefelnasr, and A. El-Shafie (2021). Developing Machine Learning Algorithms for Meteorological Temperature and Humidity Forecasting at Terengganu State in Malaysia. *Scientific Reports*, **11**(1); 1–19

Harirchian, E., V. Kumari, K. Jadhav, S. Rasulzade, T. Lahmer, and R. Raj Das (2021). A Synthesized Study Based on Machine Learning Approaches for Rapid Classifying Earthquake Damage Grades to Rc Buildings. *Applied Sciences*, **11**(16); 7540

Jiao, P. and A. H. Alavi (2020). Artificial Intelligence in Seismology: Advent, Performance and Future Trends. *Geoscience Frontiers*, **11**(3); 739–744

Mangalathu, S., H. Sun, C. C. Nweke, Z. Yi, and H. V. Burton (2020). Classifying Earthquake Damage to Buildings Using Machine Learning. *Earthquake Spectra*, **36**(1); 183–208

Mattioli, G. S., R. A. Herd, M. H. Strutt, G. Ryan, C. Widiwijayanti, and B. Voight (2010). Long Term Surface Deformation of Soufrière Hills Volcano, Montserrat from Gps Geodesy: Inferences From Simple Elastic Inverse Models. *Geophysical Research Letters*, **37**(19)

Meng, Z., C. Shu, Y. Yang, C. Wu, X. Dong, D. Wang, and Y. Zhang (2022). Time Series Surface Deformation of Changbaishan Volcano Based on Sentinel-1B SAR Data and its Geological Significance. *Remote Sensing*, **14**(5); 1213

Milczarek, W., A. Kopeć, D. Głąbicki, and N. Bugajska (2021). Induced Seismic Events Distribution of Ground Surface Displacements Based on Insar Methods And Mogi and Yang Models. *Remote Sensing*, **13**(8); 1451

Muin, B. and H. Nawir (2011). Geotechnical Aspects of the Sumatra Earthquake. *Soils and Foundations*, **51**(2); 333–341

Murwantara, I. M., P. Yugopuspito, and R. Hermawan (2020). Comparison of Machine Learning Performance for Earthquake Prediction in Indonesia Using 30 Years Historical Data. *TELKOMNIKA (Telecommunication Computing Electronics and Control)*, **18**(3); 1331–1342

Naghibi, S. A., B. Khodaei, and H. Hashemi (2022). An Integrated InSAR Machine Learning Approach for Ground Deformation Rate Modeling in Arid Areas. *Journal of Hydrology*, **608**; 127627

Oktarina, R., N. Bahagia, L. Diawati, and K. S. Pribadi (2020). Artificial Neural Network for Predicting Earthquake Casualties and Damages in Indonesia. *IOP Conference Series: Earth and Environmental Science*, **426**; 012156

Qiu, J. and X. Qiao (2017). A Study on the Seismogenic Structure of the 2016 Zaduo, Qinghai Ms6. 2 Earthquake using InSAR Technology. *Geodesy and Geodynamics*, **8**(5); 342–346

Rahardjo, P. P., A. S. Lestari, B. Wijaya, A. Lim, S. Herina, S. Rustiani, S. Wiguna, and V. Hadsari (2014). Kajian Geoteknik untuk Infrastruktur Kota Padang Menghadapi Ancaman Gempa dan Tsunami. *Research Report Engineering Science* (in Indonesia)

Sari, D. P., D. Rosadi, A. R. Effendie, and D. Danardono (2019). K-means and Bayesian Networks to Determine Building Damage Levels. *TELKOMNIKA (Telecommunication Computing Electronics and Control)*, **17**(2); 719–727

Sari, D. P., D. Rosadi, A. R. Effendie, and D. Danardono (2021). Discretization Methods for Bayesian Networks in The Case of the Earthquake. *Bulletin of Electrical Engineering and Informatics*, **10**(1); 299–307

Tapir, S., J. Yatim, and F. Usman (2005). Evaluation of Building Performance Using Artificial Neural Network: Study on Service Life Planning in Achieving Sustainability. *The Eighth International Conference on the Application of Artificial Intelligence to Civil, Structural and Environmental Engineering, Rome, Italy*, **30**

Triyoso, W., A. Suwondo, T. Yudistira, and D. P. Sahara (2020). Seismic Hazard Function (SHF) Study of Coastal Sources of Sumatra Island: SHF Evaluation of Padang and Bengkulu Cities. *Geoscience Letters*, **7**(1); 1–7

USGS (2022). *Search Earthquake Catalog. Retrieved 1st September, 2021, from Earthquake Catalog*

Usman, F. (2021). Surface Deformation of Padang City Area Induced by Over M w 5.0 Earthquake Events. *2021 International Conference on Computer Science and Engineering (IC2SE)*, **1**; 1–7

Usman, F., A. Syamsir, and J. Melasari (2022). Mapping of Earthquake-Induced Land Deformation on Urban Area Using Interferometric Synthetic Aperture Radar Data of Sentinel-1. *Recent Advances in Earthquake Engineering*. Springer; 491–502

Xie, Y., M. Ebad Sichani, J. E. Padgett, and R. DesRoches (2020). The Promise of Implementing Machine Learning in Earthquake Engineering: a State of the Art Review. *Earthquake Spectra*, **36**(4); 1769–1801

Xiong, P., L. Tong, K. Zhang, X. Shen, R. Battiston, D. Ouzounov, R. Iuppa, D. Crookes, C. Long, and H. Zhou (2021). Towards Advancing the Earthquake Forecasting by Machine Learning of Satellite Data. *Science of the Total Environment*, **771**; 145256

Zhou, F., R. Li, G. Trajcevski, and K. Zhang (2021). Land Deformation Prediction via Slope Aware Graph Neural Networks. *Proceedings of the AAAI Conference on Artificial Intelligence*, **35**; 15033–15040

